ROM SAF Report 34
Ref: SAF/ROM/METO/REP/RSR/034
Web: www.romsaf.org
Date: 21 Mar 2019

ROM SAF Report 34

An initial assessment of the quality of RO data from Metop-C

N E Bowler

Met Office, Exeter, UK

Document Author Table

	Name	***Function***	***Date***	***Comments***
Prepared by:	N E Bowler	ROM SAF Project Team	21 Mar 2019	
Reviewed by:	John Eyre	Met Office review	30 Jan 2019	
Reviewed by:	Mary Forsythe	Met Office review	12 Feb 2019	
Reviewed by:	S B Healy	ROM SAF reviewer	01 Mar 2019	
Approved by:	K B Lauritsen	ROM SAF Project Manager	20 Mar 2019	

Document Change Record

Issue/Revision	***Date***	***By***	***Description***
0.1	24 Jan 2019	NEB	1st draft
0.2	30 Jan 2019	NEB	2nd draft
0.3	13 Feb 2019	NEB	3rd draft
0.4	05 Feb 2019	NEB	4th draft
1.0	20 Mar 2019	NEB	Final version, following review by KBL

ROM SAF

The Radio Occultation Meteorology Satellite Application Facility (ROM SAF) is a decentralised processing centre under EUMETSAT which is responsible for operational processing of GRAS radio occultation (RO) data from the Metop satellites and RO data from other missions. The ROM SAF delivers bending angle, refractivity, temperature, pressure, and humidity profiles in near-real time and offline for NWP and climate users. The offline profiles are further processed into climate products consisting of gridded monthly zonal means of bending angle, refractivity, temperature, humidity, and geopotential heights together with error descriptions.

The ROM SAF also maintains the Radio Occultation Processing Package (ROPP) which contains software modules that will aid users wishing to process, quality-control and assimilate radio occultation data from any radio occultation mission into NWP and other models.

The ROM SAF Leading Entity is the Danish Meteorological Institute (DMI), with Cooperating Entities: i) European Centre for Medium-Range Weather Forecasts (ECMWF) in Reading, United Kingdom, ii) Institut D'Estudis Espacials de Catalunya (IEEC) in Barcelona, Spain, and iii) Met Office in Exeter, United Kingdom. To get access to our products or to read more about the project please go to: http://www.romsaf.org

Intellectual Property Rights

Abstract

The Metop-C satellite was launched on 7th November 2018 into a sun-synchronous polar orbit. The first radio occultations from the GRAS instrument were received less than a week after this. Level 1 data (including bending angles) have been made available from EUMETSAT Secretariat from the very beginning. The ROM SAF have processed these data and calculated refractivity profiles - these profiles have been calculated for all the bending angle profiles, including the very earliest measurements. The Level 1 and Level 2 data are being disseminated via the EUMETCast system and GTS. Operational dissemination began on the 7th March 2019.

Overall the quality of this data is very similar to that from Metop-A and B, as might be expected from systems which use the same hardware and software. Very slight differences between the satellites exist, and these will be highlighted.

Contents

1 Bending angle evaluation

During the first week of operation some satellite manoeuvres were required. This had some small effects on the quantity of data being produced, but no significant effect on the quality was observed. Nonetheless, it was advised that data before 20th November 2018 is excluded (Marquart, 2018, personal communication). Therefore only data from this date to 10th January 2019 is included in this report.

1.1 Bias and standard deviation characteristics

Figure 1.1 shows the normalised difference between the bending angle observation and the background forecast from the Met Office's operational global numerical weather prediction (NWP) model. The mean and standard deviation are calculated as

$$\mu = \frac{1}{N}\sum_{i=1}^{N}\frac{O_i - B_i}{B_i} \tag{1.1}$$

$$\sigma = \sqrt{\frac{1}{N}\sum_{i=1}^{N}\left(\frac{O_i - B_i}{B_i} - \mu\right)^2} \tag{1.2}$$

where O_i and B_i are the observed and background values for occultation i in the period, and there are N occultations overall. Figure 1.1 compares the statistics for the three Metop satellites. Reassuringly all three satellites show very similar characteristics, indicating that the instrument on Metop-C is behaving as expected. In the lower troposphere, Metop-B has a slightly smaller bias than the other two satellites. Between 50km and 60km Metop-A has a slightly smaller bias than the others.

The number of observations received from Metop-C is somewhat less than for the other satellites. The Met Office received 4.3% fewer observations for Metop-C than for Metop-B, compared with a difference of 0.6% for Metop-A. This is mostly caused by problems in the data reception at the Met Office for data from Metop-C, since this data reception is not operational. However, after quality control we received 6.6% fewer observations from Metop-C than Metop-B, and 2.6% few observations for Metop-A than Metop-B. Therefore the quality control is rejecting 2% more observations for both Metop-A and C than for Metop-B. It is not clear why this is the case.

The difference between rising and setting occultations is shown in Figure 1.2. The large bias seen in all lower-tropospheric Metop bending angles is due to a bias in the setting bending angles. The bias is slightly smaller for Metop-B in both the rising and setting bending angles, and this leads to a smaller overall bias. It is notable that the standard deviation is also larger for setting measurements in this region.

Figure 1.3 shows the bias and standard deviation, as Figure 1.1, but separated by different latitude ranges. The Figure compares Metop-C with Metop-A, as the instruments on these satellites appear to be performing very similarly. There is no clear difference between these satellites, except that Metop-C has slightly fewer observations as described above.

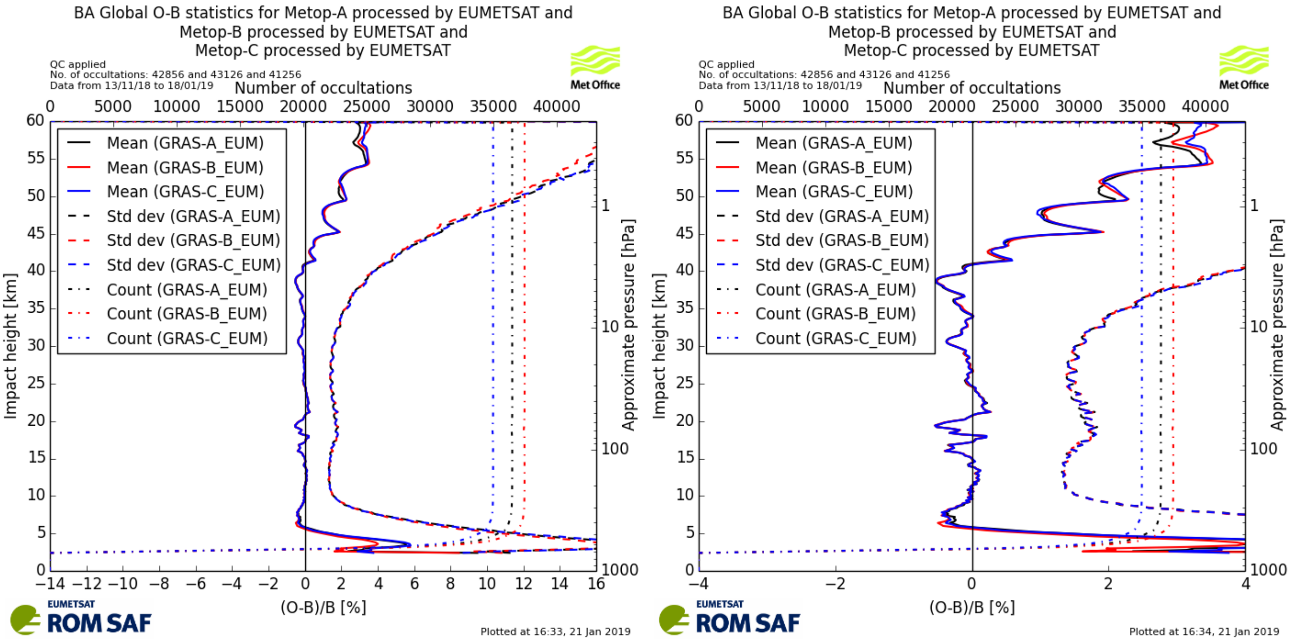

Figure 1.1: The bias and standard deviation of the normalised difference between the observation and the NWP model background forecast $(O-B)/B$ for bending angle. (left) Graph with a scale showing the full range of data, (right) graph with zoom to highlight the performance between 10 and 40km.

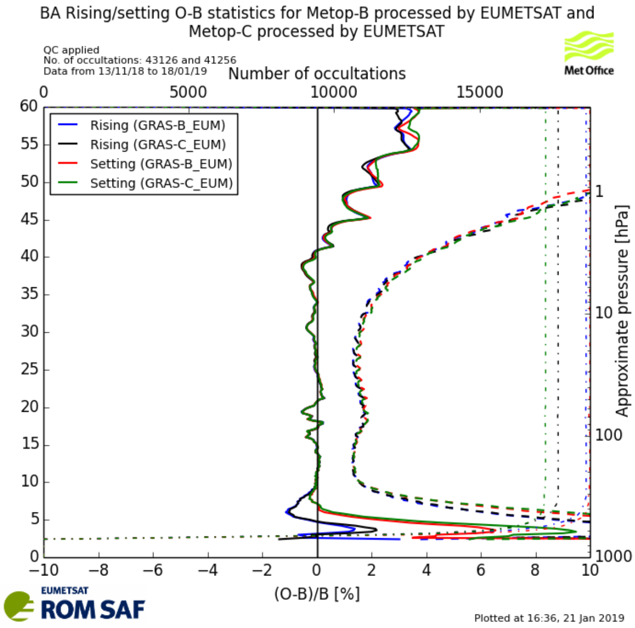

Figure 1.2: Data from rising and setting occultations, for Metop-B and Metop-C. The bias and standard deviation of the normalised difference between the observation and the NWP model background forecast $(O-B)/B$ for bending angle.

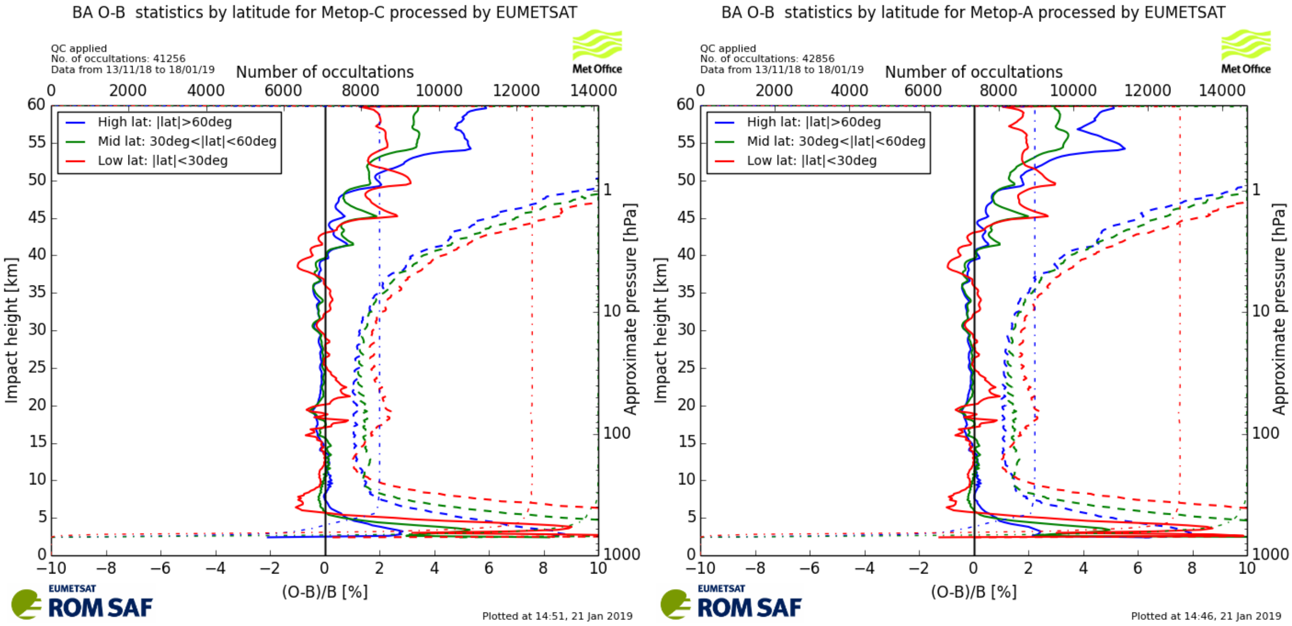

Figure 1.3: The bias and standard deviation of the normalised difference between the observation and the NWP model background forecast $(O-B)/B$, separated by different latitudes for bending angle.

1.2 Vertical correlations

When bending angle data is assimilated into the Met Office's NWP system it is assumed that the error in each bending angle measurement is independent of the errors in every other measurement. Therefore we would like the vertical observation-error covariance matrix $\mathbf{R}$ to be diagonal, and the vertical correlations of $O-B$ (which corresponds to the covariance matrix $\mathbf{B}+\mathbf{R}$) to be close to diagonal, containing only the correlations from the background-error covariance matrix. Figure 1.4 shows the vertical correlation of the normalised difference between the observation and NWP model background forecast for Metop-A and C. Due to the way that bending angle is calculated as a smoothed difference between Doppler shifts, we expect a region of positive correlations near the diagonal, and negative correlations at further distances. As before there are only very slight differences between Metop-C and Metop-A. There is a suggestion that the vertical correlations in the troposphere are slightly shorter range with Metop-C. It is not clear if this is a statistically significant difference.

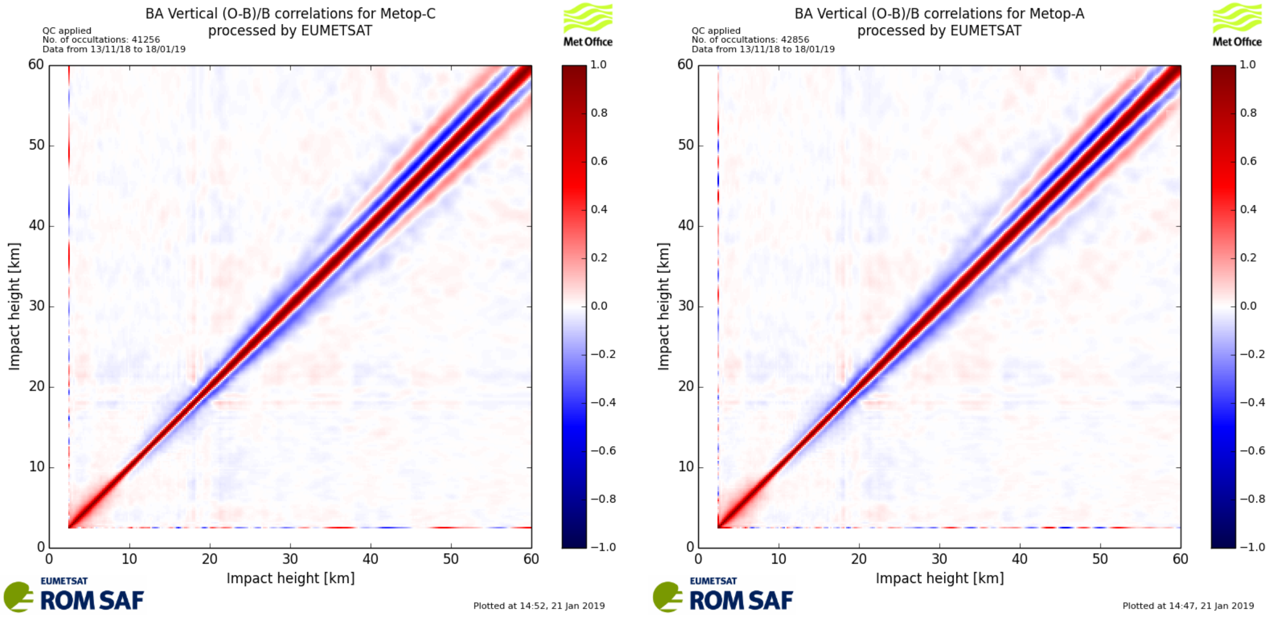

Figure 1.4: Vertical correlations of normalised differences between the observation and the NWP model background for bending angle.

2 Refractivity assessment

Measurements of refractivity are calculated from the bending angle for the ROM SAF by the Danish Meteorological Institute (DMI). Detailed assessments of the refractivity measurements will be published by DMI, so only a brief summary of the main points is presented here. Figure 2.1 shows the mean and standard deviation of normalised differences between the observed refractivity and that produced by the NWP model forecast. The similarity between the data for the three satellites is once again remarkable. Metop-C appears to have slightly larger standard deviations above 50km.

Once again Metop-C has fewer observations than the other two satellites (2% less than Metop-B, compared with a 0.7% reduction for Metop-A). However, there were not the same transmission issues for refractivity data as were experience for bending angle data. Metop-A has lower biases than Metop-B and C above 50km. This is consistent with the result seen for bending angle. It is not clear what causes the difference in bias.

The vertical correlation of the difference between modelled and observed refractivity are shown in Figure 2.2 for Metop-A and C. These satellites show very similar vertical correlations and there is little to differentiate the two.

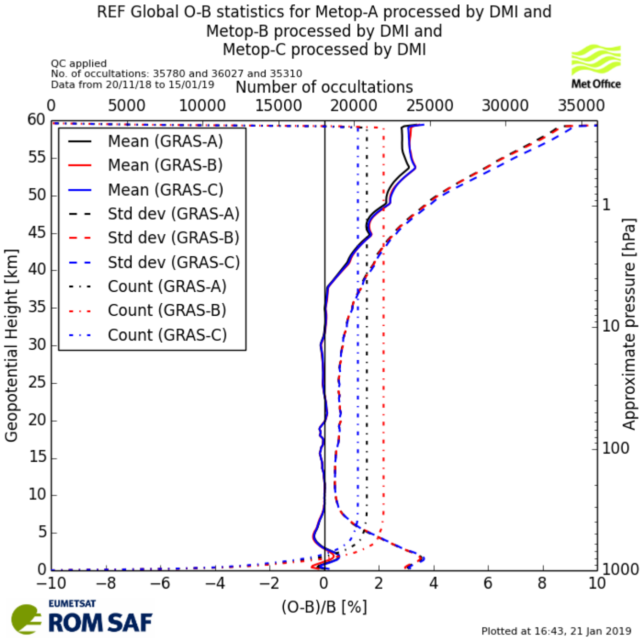

Figure 2.1: The bias and standard deviation of the normalised difference between the observation and the NWP model background forecast $(O-B)/B$ for refractivity.

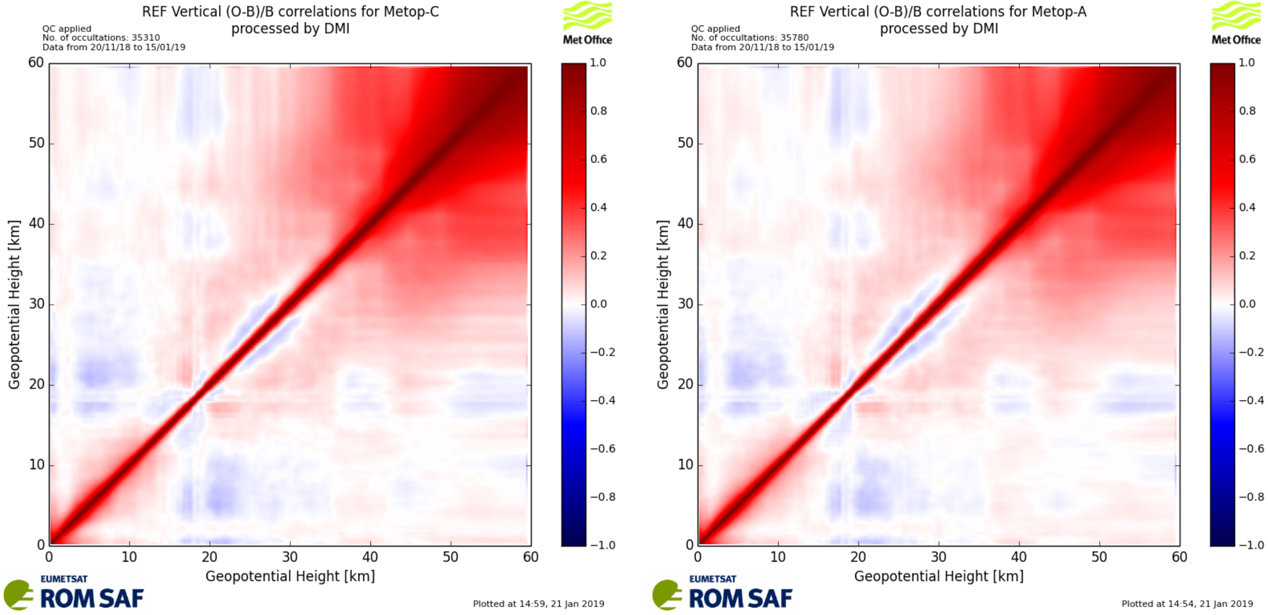

Figure 2.2: Vertical correlations of normalised differences between the observation and the NWP model background for refractivity.

3 Other notable features

The timeliness of the data, as received via EUMETCast is very good. The average time taken for an observation from Metop-C to be received at the Met Office is 98 minutes, which compares with 85 minutes for Metop-A. Given that Metop-C is not operational this is very good timeliness. The timeliness for Metop-B is better than that for Metop-A and C because it uses a satellite downlink in the Antarctic which is not available for the other satellites.

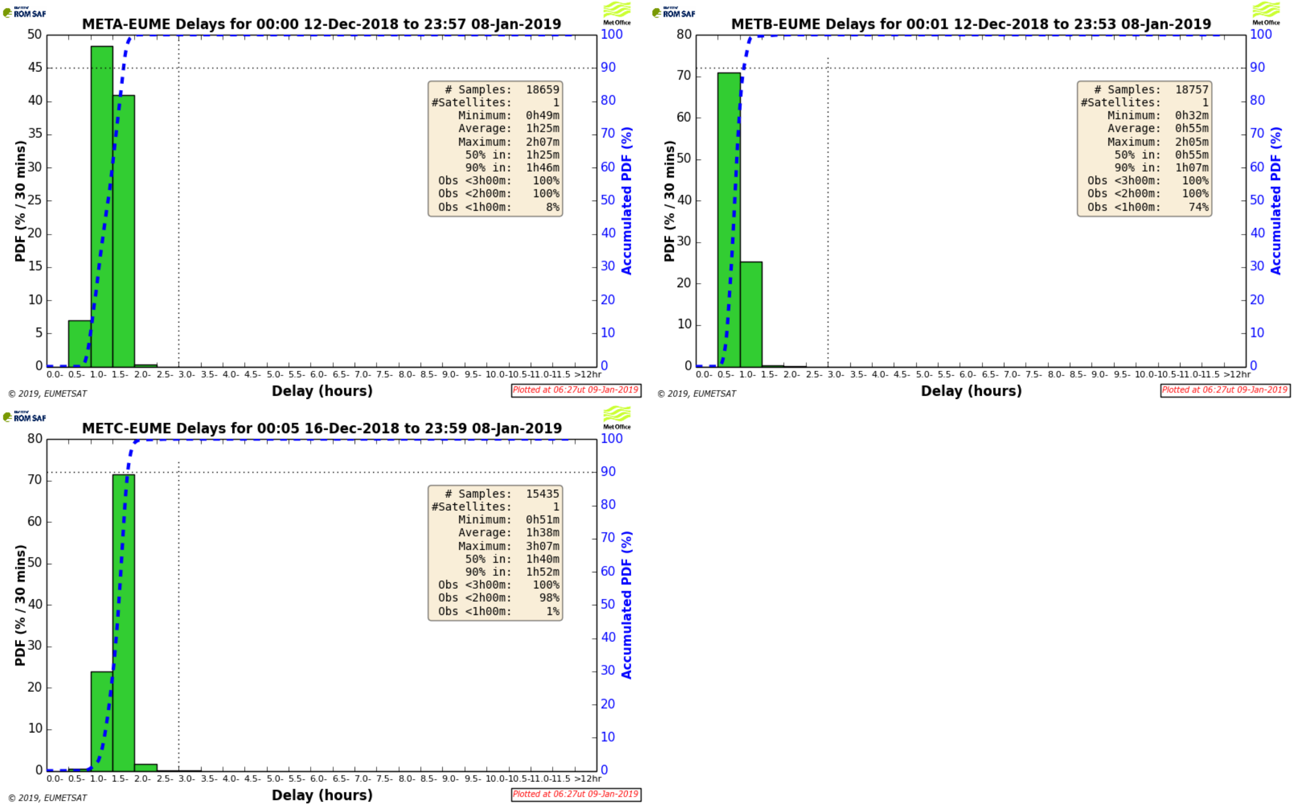

Figure 3.1: Time delay in receiving the occultations, as calculated from the receipt time in the Met Office's observations data base.

4 Conclusion

The overall quality of the data from Metop-C is very similar to that from Metop-A and B. This is to be expected since each satellite uses the same hardware and software. Metop-C produces slightly fewer observations than Metop-A, which produces slightly fewer observations than Metop-B. Metop-B has slightly smaller bending angle biases in the troposphere than Metop-A and C. Metop-A has slightly smaller biases in bending angle and refractivity above 50km. The standard deviation of Metop-C refractivity error is slightly larger the other satellites above 50km. Given the large similarities with existing data sources and the stability of the data feed it began to be assimilated into the Met Office's operational NWP system on 19th March 2019.

ROM SAF (and earlier GRAS SAF) Reports

SAF/GRAS/METO/REP/GSR/001	Mono-dimensional thinning for GPS Radio Occulation
SAF/GRAS/METO/REP/GSR/002	Geodesy calculations in ROPP
SAF/GRAS/METO/REP/GSR/003	ROPP minimiser - minROPP
SAF/GRAS/METO/REP/GSR/004	Error function calculation in ROPP
SAF/GRAS/METO/REP/GSR/005	Refractivity calculations in ROPP
SAF/GRAS/METO/REP/GSR/006	Levenberg-Marquardt minimisation in ROPP
SAF/GRAS/METO/REP/GSR/007	Abel integral calculations in ROPP
SAF/GRAS/METO/REP/GSR/008	ROPP thinner algorithm
SAF/GRAS/METO/REP/GSR/009	Refractivity coefficients used in the assimilation of GPS radio occultation measurements
SAF/GRAS/METO/REP/GSR/010	Latitudinal Binning and Area-Weighted Averaging of Irregularly Distributed Radio Occultation Data
SAF/GRAS/METO/REP/GSR/011	ROPP 1dVar validation
SAF/GRAS/METO/REP/GSR/012	Assimilation of Global Positioning System Radio Occultation Data in the ECMWF ERA-Interim Re-analysis
SAF/GRAS/METO/REP/GSR/013	ROPP PP validation
SAF/ROM/METO/REP/RSR/014	A review of the geodesy calculations in ROPP
SAF/ROM/METO/REP/RSR/015	Improvements to the ROPP refractivity and bending angle operators
SAF/ROM/METO/REP/RSR/016	Simplifying EGM96 undulation calculations in ROPP
SAF/ROM/METO/REP/RSR/017	Simulation of L1 and L2 bending angles with a model ionosphere
SAF/ROM/METO/REP/RSR/018	Single Frequency Radio Occultation Retrievals: Impact on Numerical Weather Prediction
SAF/ROM/METO/REP/RSR/019	Implementation of the ROPP two-dimensional bending angle observation operator in an NWP system
SAF/ROM/METO/REP/RSR/020	Interpolation artefact in ECMWF monthly standard deviation plots
SAF/ROM/METO/REP/RSR/021	5th ROM SAF User Workshop on Applications of GPS radio occultation measurements
SAF/ROM/METO/REP/RSR/022	The use of the GPS radio occultation reflection flag for NWP applications
SAF/ROM/METO/REP/RSR/023	Assessment of a potential reflection flag product
SAF/ROM/METO/REP/RSR/024	The calculation of planetary boundary layer heights in ROPP
SAF/ROM/METO/REP/RSR/025	Survey on user requirements for potential ionospheric products from EPS-SG radio occultation measurements

ROM SAF (and earlier GRAS SAF) Reports (cont.)

SAF/ROM/METO/REP/RSR/026	Estimates of GNSS radio occultation bending angle and refractivity error statistics
SAF/ROM/METO/REP/RSR/027	Recent forecast impact experiments with GPS radio occultation measurements
SAF/ROM/METO/REP/RSR/028	Description of wave optics modelling in ROPP-9 and suggested improvements for ROPP-9.1
SAF/ROM/METO/REP/RSR/029	Testing reprocessed GPS radio occultation datasets in a reanalysis system
SAF/ROM/METO/REP/RSR/030	A first look at the feasibility of assimilating single and dual frequency bending angles
SAF/ROM/METO/REP/RSR/032	An initial assessment of the quality of RO data from KOMPSAT-5
SAF/ROM/METO/REP/RSR/033	Some science changes in ROPP-9.1

ROM SAF Reports are accessible via the ROM SAF website: http://www.romsaf.org